Study of Magnetoresistance in multilayer Ta/NiFe/Ta structure and in Ta/CoFe/NiFe/Cu/CoFe/MnIr/Ta spin valve.

H. J. Nóbrega

April 2018

Abstract

The Giant Magnetoresistance (GMR) of a spin valve was studied for angular variation, with a maximum of about 7.3% for a configuration of colinear current and applied field, and a minimum of about 1% for the perpendicular configuration. A model for the GMR was tested and confirmed with $r^2 = 0.993$ and an error of 10.65%. From that study, the angular variation of coupling field was determined, with minimum of 14.9 Oe, for current and field alligned, and maximum of 21.54 Oe. Sensibility was studied as a function of H and $\theta_{\vec{j},vecH}$. The global maximum was for $\vec{j}$ and $\vec{H}$ antiparalell.

The Anisotropic Magnetoresistance (AMR) of a thin film was found to be, at most, 0.25%, for $\theta_{\vec{j},\vec{H}} = 22.5°$. A model for AMR was unsuccessfully tested with $r^2 = 0.347$, suggesting possible non-coplanarity between remanent $\vec{M}$ and the horizontal plane of the sample. Sensibility was analogously studied, with a maximum for 22.5°, suggesting a non-zero angle between the easy axis and $\vec{j}$ (unconclusively tested with zero-field resistances measurements for $\vec{j}$ along different directions in the sample).

A sensing application was tested, showing qualitatively promising results, with no further calibration being pursued for technical issues.

1 Introduction

1.1 Spin valves, a nanostructure with Giant Magnetoresistance (GMR)

The Nobel Prize in Physics of 2007 was awarded to Albert Fert and Peter Grünberg for their discovery of an essentially quantum effect which occured in laboratory grown materials of nanometric characteristic dimensions. As a magnetoresistive effect, it arises when a magnetic field influences the transport properties of electrons in those layered materials, especially by means of an interaction between their magnetization and the spin of the carriers, the basis of what is known today as spin electronics, or spintronics.

GMR lead to a significant improvement in lifestyle of the modern society, either in magnetic field sensing by means of spin valves – namely, for automotive industry and biomedical technology [6] – and information storage devices, such as hard-disk read heads or magnetic random-acess memories (MRAM) [2].

The spin valve, an example of which is shown in Fig.1, is a nanostructure exhibiting GMR, tipically composed of several layers, which may be formed by chemical deposition over a substrate of silicon (glass). As the growth of a metallic layer over glass is usually carried out with an amorphous structure, a sacrifice layer of tantalum (Ta) is often deposited over silicon, so that crystaline layers may be grown over it.

The first layer is composed of two metallic alloys, each one with a desirable specification (low coercivity and high magnetic polarization), that behave as one ferromagnetic layer, having those two properties, as a result of a trade off, so recurrent in nanoscience. Above these layers is deposited a magnetically non-responsive material, such as copper (Cu), with high

conductivity.

What follows is again a dual layer, composed of a ferromagnetic material and an antiferromagnetic one. It so happens that the latter is responsible for a shift of $H_{exch.}$, the exchange field, in the horizontal scale of the hysteresis loop of the former, thus "pinning" its magnetization even for relatively high values of H, for which it would be expectable that the magnetic momenta allignment had already occured. The physical ground for such pinning is the existance of an exchange angular momentum between the two sublayers which couples their magnetizations.

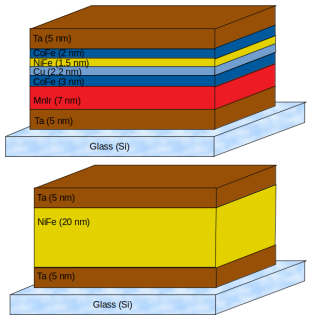

Figure 1: Composition of two nanostructures with magnetoresistance properties. In the top, the several components of a spin valve are presented, from bottom to top, respecting the order in which their contributions to the structure were mentioned . In the bottom, the composition of a multilayer thin film composed of a ferromagnetic material.

Finally, a protective layer of a non-oxidating metal may be grown on top of the structure described, with the purpose of preventing any eventual oxidation.

These structures have been studied in recent years, and a propper characterization is essential for the constitution of calibration curves for sensing applications. The GMR can be analysed in terms of its angular dependence, in the sense that the flow of electrons may occur at an angle $\theta_{\vec{j},\vec{M}} \neq 0$ with the magnetization of the fixed layer. If that is the case, the magnetoresistance will be smaller than the one for $\theta_{\vec{j},\vec{M}} = 0$, ΔR, and given by [4]

$$R(\theta) = R_0 + \Delta R \cos^2 \theta_{\vec{j},\vec{M}}/2, \qquad (1)$$

where R_0 refers to a base level for resistance imposed by the low resistance level for $\theta_{\vec{j},\vec{M}} = 0$.

1.2 Anisotropic Magnetorresistance (AMR) in multilayer structures.

Another magnetoresistive effect that has an important expression in multilayer structures, even if it is about 1000 times less important than GMR, is the AMR. The layout of one possible nanoscale structure, exhibiting AMR, and which was available for testing in the laboratory, is depicted in Fig.1.

Following the work of Thomson (1857), spin-orbit coupling relates those two angular momenta intrinsic of the electron and introduces anisotropy in the measurement of the resistance of a homogenous ferromagnetic material as a function of the angle between magnetization and direction of electron flow. The contribution of $\theta_{\vec{M_{sat.}},\vec{j}}$ is preponderant, compared to the thermal variation of magnetization [3].

The anisotropic magnetorresistance may be expressed by means of the semiempirical relation expressed in Eq.2, where R refers to the value of resistance measured for a value of H sufficiently high for the magnetization to be saturated, that is, completely alligned with $\vec{H}$. If that is the case, then the angle $\theta_{\vec{j},\vec{M_{sat.}}}$ is equal to the one between $\vec{H}$ and $\vec{j}$.

$$R(\theta) = R_\perp + \Delta R \cos^2 \theta_{\vec{j},\vec{M}}, \Delta R \equiv R_\parallel - R_\perp. \qquad (2)$$

By inspection of the equation above, one also concludes that $R_{\parallel,\perp}$ is the saturated resistance measured when the current is paralell (transverse) to $\vec{H}$.

2 Experimental preparation for the study of the spin valve.

Previously to proceeding with measurements, a degree of freedom had to be eliminated, that which consisted of the angle between $\vec{j}$ and the easy axis of the free layer. The specifications of the structure were such that the remanent magnetization was oriented along the longitudinal direction, therefore the easy axis may be considered to be alligned with the

four contacts and with $\vec{j}$. The validation of this assumption is provided below, with the agreement of experimental data, up to the contribution of uncertainty due to the inaccurate measurement of the angle $\theta_{\vec{j},\vec{H}}$.

For this investigation, the setup depicted in Fig.2 was used. It consists of a set of two coils in the Helmholtz configuration, designed to obtain an approximately constant $\vec{H}$ in the periaxial region, where the samples were placed. In order to measure the resistance of the structures, the four contact method was employed [1], which briefly consists of measuring voltage drop and current intensity along the direction defined by the contact points – in the present case, charge carriers will flow in the direction of $\vec{j}$ and paralelly to each of the strucures' layers.

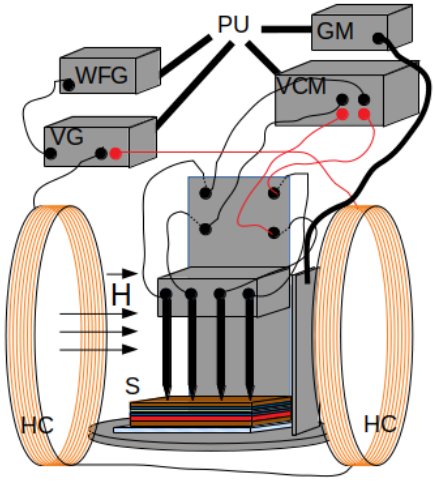

Figure 2: Setup used for the measurements of magnetoresistance in spin valve and multilayer structure, comprising the Helmholtz coils (HC), waveform generator (WFG), gaussmeter (GM), voltage and current measurement device (VCM), processing unit (PU) and sample (S). This figure is not to scale (4 contacts are zoomed in, as well as the sample).

For a given orientation of $\vec{j}$ and $\vec{H}$, the field intensity was varied by a LabView routine, that automatizes the process and measures the voltage drop as described, while the current is kept approximately constant, providing a direct measurement of the resistance. The variation of H is performed in a step-like manner, and not with the aid of a waveform – as in, for example, a MOKE setup [7] –, for the timescale of the domain reorientation is not compatible with the high frequency of a waveform. Therefore, the waveform generator shown in the setup is kept at DC level.

The control of the applied field was not performed via the LabView routine, but with the aid of a gaussmeter.

The variation of the angle $\theta_{\vec{j},\vec{H}}$ was performed manually, in the sense that only a rough visual estimate of the several orientations was performed.

3 Discussion of obtained results.

3.1 Giant Magnetorresistance of a spin valve.

3.1.1 Magnetic resistance for the allignment of H with the easy axis of the spin valve.

In Fig.3, it is shown the variation of the curves that characterize the resistive behaviour of the spin valve with the angle $\theta_{EA,\vec{H}}$ between the easy axis and the applied magnetic field.

The case of $\theta_{EA,\vec{H}} = 0^o$ is an academic example. The obtained results seem to agree with an hysteresis loop, namely, that of the magnetization as a function of the applied magnetic field. They may be understood by reasoning that, as electrons flow through the layers of the spin valve, from left to right, there is a probability of scattering by the atoms in the lattice, whose magnetic momenta are directed preferencially in the direction of the easy axis, and that is directly linked to the resistance felt by those charge carriers.

The pinned layer will retain its magnetization independently of H – say, pointing right – whether the free layer will not, and two configurations are possible: both magnetizations being paralell or antiparalell. Now, the probability of scattering is higher when the spins of electrons have the direction opposite to that of the angular momenta of the lattice.

That being said, it should be true that both magnetizations paralell to the spin will result in a least resistance configuration, the opposite being also true. That is the reason why the resistance follows the hysteresis loop of the magnetization versus the field intensity, as seen in Fig.3, for $\theta_{EA,\vec{H}} = 0^o$.

3.1.2 Angular dependence of the magnetic resistance in the spin valve.

In order to understand all the other results shown in Fig.3, at least qualitatively, it suffices to think of the conducting electrons as an ensemble of all possible spin orientations. The case of a spin alligned with the natural magnetization axis of a sample has already been analysed.

Now, as there is a small angle between the applied field and the hard axis, there are electrons for which the spin projection onto this new rotated axis is positive or negative. For sufficiently small magnetic excitation field, it is true that the CoFe-MnIr component will keep its magnetization, for which the electrons with spin pointing, say, left and right are most sensitive to. So, on average, there are two spin orientations that represent maximum resistance, and the resistance tends to increase especially as the magnetic field increases also, and the tendency of the magnetic moments to reallign with the field. However, as the field is progressively increased, the pinned layer becomes itself free and tends to allign with the magnetization, just as the free layer was doing. The probability of allignment for a magnetic moment increases with the magnetic field, and, as the field becomes strong enough, all "pinned" and "free" momenta are alligned and one recovers a situation of minimum resistance, equivalent to that of null field, except for momenta orientation.

The coupling magnetic field is another important information which can be extracted from the magnetization loop, since it corresponds to the shift in the resistance loops. In Fig.4 it is shown that the coupling field intensity is maximum for antiparalell $\vec{j}$ and $\vec{H}$.

This reasoning does not depend on the sign of H only for a perfect orientation of that field along the hard axis of the ferromagnetic material. In fact, if

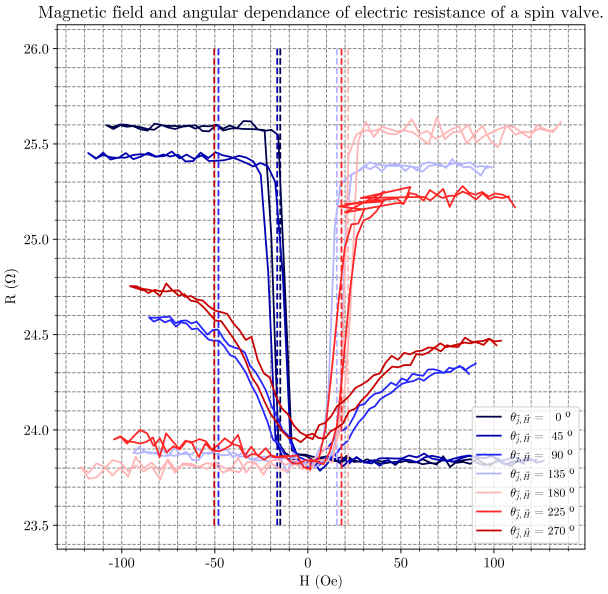

Figure 3: Spin valve resistance curves as a function of the angle between the line containing the four contacts and $\vec{H}$. The dashed lines refer to the coupling field extracted from each of the loops.

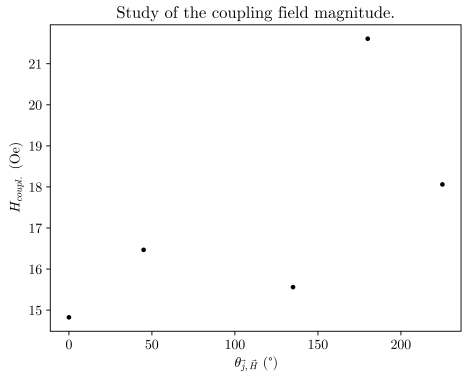

Figure 4: Coupling fields studied for all orientations. It should be noted that for orientations sufficiently close to transverse field and current the coupling field can not be determined from the curves shown and their range in studied field magnitudes.

there is a small asymmetry, the resistance will increase slightly more for one of the possible signs. That is due to the commulative effect of an hysteretic response, as there is a component of $\vec{H}$ paralell to the remanent magnetization.

3.1.3 Quantitative parameters for the magnetoresistance analysis.

The explanations of the shape of the curves given in the previous section are complemented by Eq.1 – in order to describe the variation of the high-resistance state in all configurations concerning the angle $\theta_{\vec{H},\vec{j}}$, the plotting of the expected curve is shown alongside data points in Fig.5.

The quality of the fit is quantitavely interesting, and shows that the spin valve behaves as predicted, up to uncertainty in the measurements. There is also good agreement of the data for complementar angular values, as is seen in Fig.3, where parity about the resistance axis can be verified for saturation data, as symmetric values of the applied field should yield the same physical conclusions.

Another important conclusion is that it appears that there is no angle between $\vec{j}$ and the easy axis of the free layer of the structure, as the reasoning detailed in the previous section is strongly dependant of this assumption and the curves are easily explained by such reasoning (again, up to uncertainty in the angle).

Another study that was performed was that of the sensibility of the apparatus, defined as $S = \partial_H R$. As seen in Fig.6, the sensibilities were found to be greater near the transition zones in the loops, which is connected to the operation within the coercivity of the free layer. As the magnetization is allowed to fluctuate due to the low intensity of $\vec{H}$, the movement of domain walls in the attempt of energy minimization through containment of demagnetization energy has an average effect over the scattering of electrons of much bigger magnitude than when magnetization is saturated.

In terms of angular dependance, it can be seen that the smallest sensibilities appear at angles of 90° and 270°, meaning a much smoother trace of the curve, which is itself linked to the fact that magnetization is

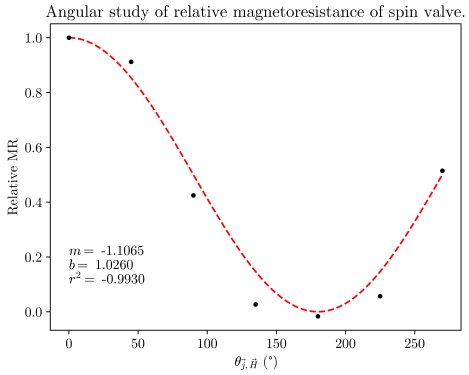

Figure 5: Magnetoresistance – by definition, the normalized variation of resistance in the spin valve –, for the application of $\vec{H}$ at different angles in relation to $\vec{j}$. Also shown are the fitting parameters for a linear regression in the form $y = mx + b$, where $y = \frac{R-R_0}{\Delta R}$ and $x = \cos^2 \theta_{\vec{H},\vec{j}}/2$.

an approximately linear of the non-saturating magnetic field, if the latter is alligned with the hard axis.

Finally, the ratio $\Delta R/R_{min}$ was computed, in order to have an idea of the percentual order of magnitude of this effect. For that, for each angle tested, the difference in resistance between the two saturated cases ΔR was computed, and divided by the minimum saturation resistance, yielding the graphic in Fig.7.

It is possible to conclude that the percentual variation due to GMR is quite accountable, and will be seen to represent about 100 times more significance than AMR.

3.2 Study of the resistive behaviour of a multilayer structure.

The experimental setup used was the same of Fig.2, only changing the sample that was analysed.

3.2.1 Curves of variation of resistance with magnetic field.

The first measurements were those of the magnetoresistance as a function of the applied magnetic field,

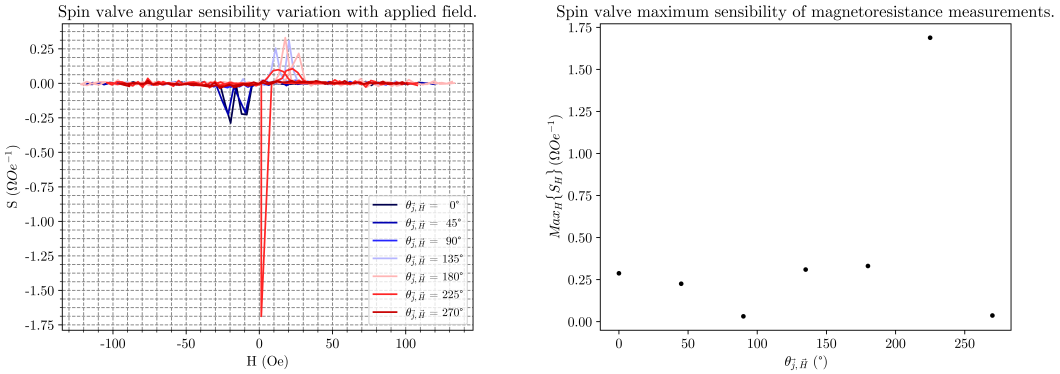

Figure 6: On the left, sensibilities of the spin valve for several values of applied field and angle between the direction of the current and of the applied magnetic field. On the right, the plot of the maximum sensibility for each angle, in absolute value.

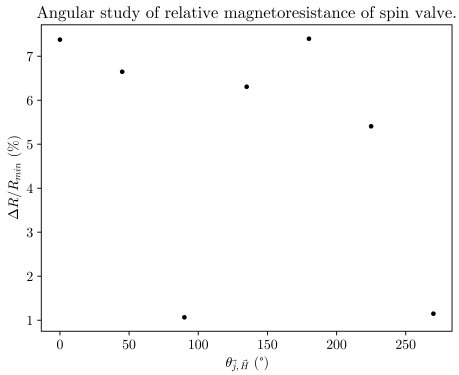

Figure 7: Plot of the relative GMR for each of the angles tested.

as in Fig.8.

Please note that the labels of the curves correspond to the angle $\theta_{\vec{j},\vec{M_{sat}}}$, where $\vec{M_{sat}}$ denotes the saturation magnetization. Thus, $\theta_{\vec{j},\vec{M_{sat}}} = \theta_{\vec{j},\vec{H}}$, i.e., the angle of which the sample was rotated about its normal vector, clockwise. It does not, necessairely, correspond to the angle between the easy axis of the sample and the applied $\vec{H}$ field.

As first remarks, it is important to check that the saturation magnetization is not recovered for complementary angles, which may support the idea that the magnetization is not paralell to the plane of the film, due to irregularities in the deposition process.

3.2.2 Quantitative parameters for the magnetoresistance analysis.

Firstly, the anisotropic magnetoresistance was computed and normalized. The tendency shown in Eq.2 was not verified, as is visible in Fig.9. Despite of the weak global fitting, it is true that for angles smaller than 90°, the data follows the predictions of the model in Eq.2 with an r^2 of 0.956 and an error of about 14.6%. There is, however, no physical basis for the elimination of the other data points.

The behaviour of the sample appears to be sensitive to orientation, yielding a magnetoresistance which is different for complementary angles. The con-

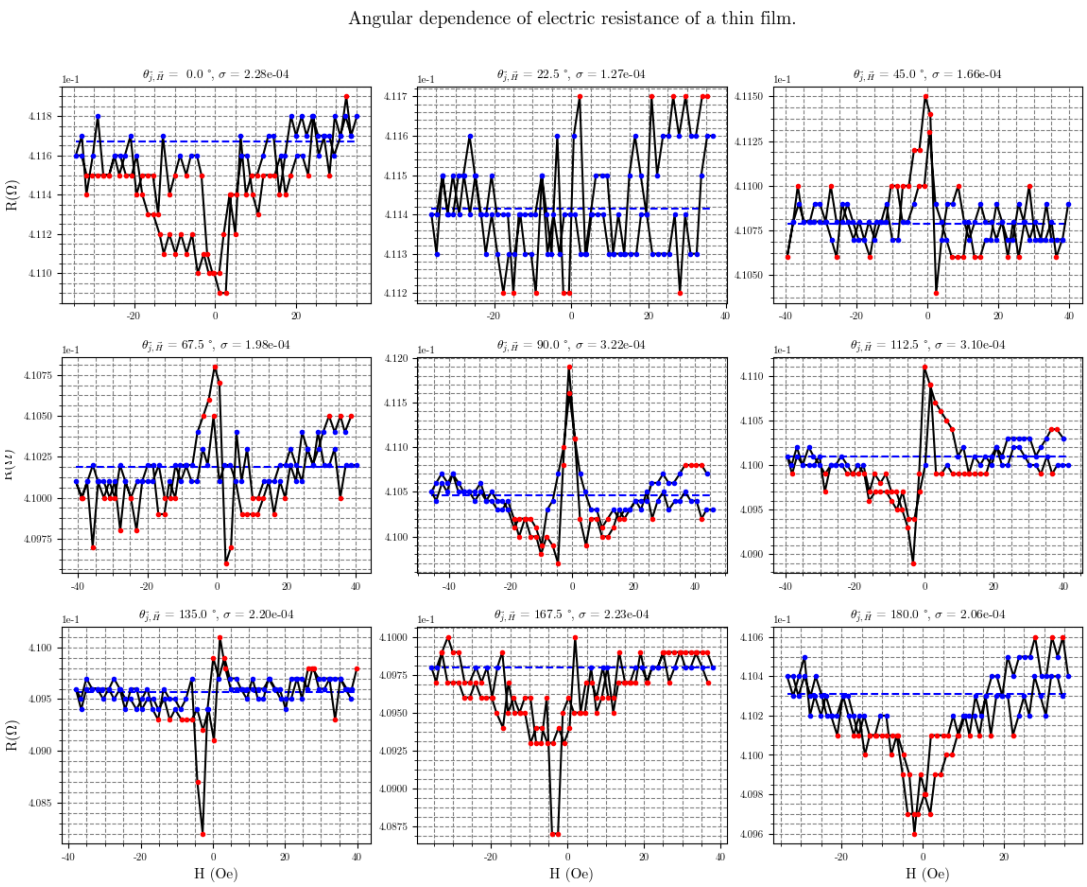

Figure 8: Variation of the resistance curves with the applied field intensity for several configurations of the thin film in the setup. In blue, are shown the experimental points used to compute the saturation resistance, shown in the dashed line, as the mean of that data set, whose standard deviation is computed and shown in the title of each subplot.

ditions of measurement for the data series represented were not altered during the experiment, and Joule variation of resistance does not appear to be significative, as the saturation resistances globally appear to coincide.

The appearance of the curves for angles greater than 90° is not very discrepant, roughly speaking, to that of curves that follow the empirical law in Eq.2.

The setup has no appreciable changes for the trials regarding angles greater than 90°. Therefore, it is plausible that the sample itself does not behave as expected. The sensitivity to the relative direction of the magnetic field and current is usually connected to giant magnetorresistance, as seen in the spin valve in Fig.5, so that it may be possible that a subsidiary effect of that nature might be lowering the expected results for resistance, with greater expression for angles closer to 180°.

Another possible analysis is the extraction of the magnetoresistance ratio, which describes, in absolute

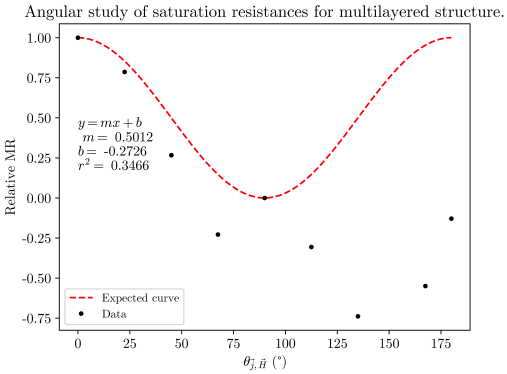

Figure 9: Study of AMR: both the resistance predicted by Eq.2 and the measured data are plotted. Also shown are the fitting parameters for a linear regression in the form $y = mx + b$, where $y = \frac{R-R_0}{\Delta R}$ and $x = \cos^2\theta_{\vec{H},\vec{j}}$.

value, the variation in resistance relative to the null-field resistance. As seen in Fig.10, the AMR, for this sample, has a maximum expression of about 0.25%, for a configuration of field perpendicular to current, the minimum value occuring for 22.5°, which corresponds to the almost absence of this effect in the sample. This may be connected to an angular deviation between $\vec{j}$ and the easy axis of the sample, as will be seen later, since we would be expecting the minimum to occur for the easy axis alligned with $\vec{j}$ and $\vec{H}$.

A similiar calculation of sensibility, as described for the study of the spin valve, was performed. It was chosen not to show the plots of sensibility for each of the angles studied, and as a function of H, for a matter of space. However, the maximum sensibility is shown for each angle in Fig.11.

The fact that the sensibility is higher for the angle of 22.5° might indicate that there is a non-null angle between the easy axis of the sample and the direction of current, an extra degree of freedom that had to be determined.

Another evidence may be taken from Fig.8. In fact, it suffices to reason that, if $\vec{H}$ is along the easy axis (EA), the angle $\theta_{\vec{j},\vec{M}}$ takes only the values $\theta_{\vec{j},EA}$ and $\pi - \theta_{\vec{j},EA}$, both having the same squared cosine. It is, therefore, to expect a negligible variation of the resistance with the applied field intensity.

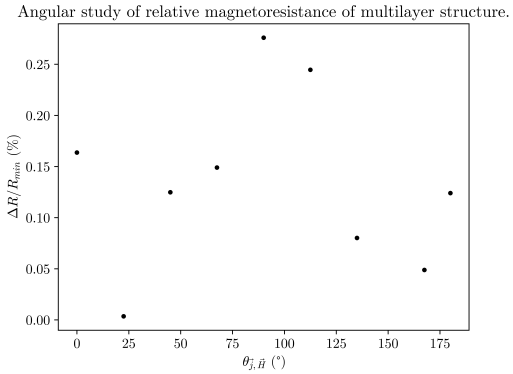

Figure 10: Study of AMR ratio, defined as the ratio between the absolute value of the maximum deviation of resistance from zero-field resistance R_0, and R_0.

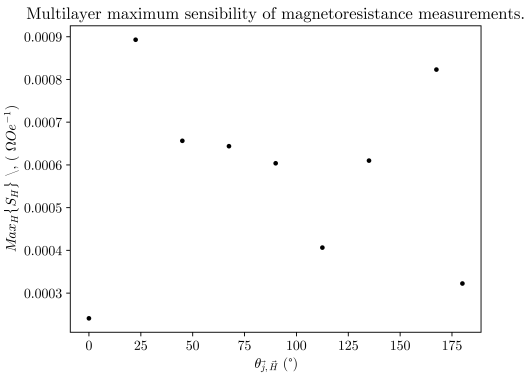

Figure 11: Plot of the maximum sensibility, in absolute value, of the multilayer structure.

By inspection of the curves $R(H)$ for different roations of the sample about its normal vector, it was straightforward to associate the angle corresponding to the curve with the least standard deviation to the one between the easy axis and $\vec{j}$.

3.2.3 Determination of the easy axis of the sample.

Further experiment was conducted in order to validate the reasoning in Sec.3.2.2. The procedure was the following: eeping the magnetic field $\vec{H}$ zero, a curve $I(V)$ was obtained from the LabView routine for several directions of $\vec{j}$ along the plane of the sample.

The determination of resistances was performed by a method of linear fitting of the experimental curve of current intensity as a function of applied voltage, yielding, for all cases, a fitting r^2 sufficiently close to one.

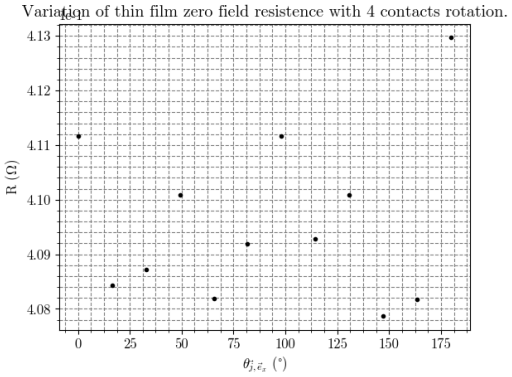

Figure 12: Null-field sample resistance for several current orientations along the plane of the multilayer structure.

The results, as shown in Fig.12, are inconclusive. This may be related to the lack of sensibility in the measurement of the rotation angle. Another possiblity migh be that the remanent magnetization is not entirely contained within the plane of the sample.

3.3 Mapping of an unknown magnetic field from magnetorresistance measurements.

For this experiment, the spin valve which was previously characterized was used to determine the magnitude of the magnetic field felt at a point at a variable distance from a permanent magnet. The first data set that was measured became corrupt after measurements for three distances, as the connection between the voltmeter and the sample was lost and had to be reestablished. The second data set was not used as well, since the sample broke in two separate pieces along the direction transverse to $\vec{j}$. The third data set was obtained from one of the two pieces marked with an X for further reference.

The experimental setup was partially adapted from the previous ones showed. As the magnetic field is now unknown, the two coils were removed from the setup shown in Fig.2. The magnet was placed along the axis where the magnitude of the $\vec{H}$ field is more significant. For that, previous testings with a gaussimetre were conducted prior to the experiment, providing the confirmation that there was expected magnetoresistance from the range of $\vec{H}$ produced by the magnets.

The procedure consisted of selecting a test distance at which to place the magnets, along a given axis determined as described above. Using a subroutine in the LabView program available to produce several measurements, namely, 43, for a fixed distance, data points consisting of measured voltages were extracted, allowing a computation of the resistance. The processing consisted of extracting the mean value and the standard deviation of that set of data points, which may be checked in Fig.13.

The sample was placed in a manner such that $\vec{j} \perp \vec{H}$. This was done in order to assure a smooth variation of resistance with the field intensity felt by the valve. Given the range of the fields tested, always controlled by a gaussimetre, it is expected that the resistivity of the sample increases with the field intensity, i.e., decreases with distance to the magnets, which is readily checked in Fig.13.

The next step would be a determination of a calibration curve which would allow a conversion be-

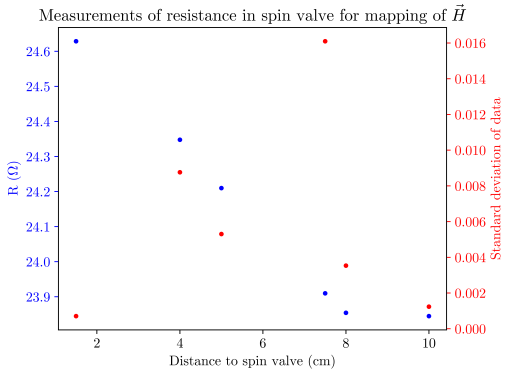

Figure 13: Resistance of the spin valve measured keeping the test magnets at several distances, and standard deviation for error analysis.

tween measured resistance and magnetic field intensity. That could not be done, given that the sample used so far had disappeared by the time those measurements were to be made.

4 Conclusive remarks

The spin valve was analysed in terms of its GMR, investigated for several values between the applied field and current. The variation of magnetoresistance following a semi empirical $\cos^2 \theta_{\vec{j},\vec{H}}/2$ law was quantitatively verified, with an r^2 of 0.993. The variation curves showing the evolution of the two, low and high resistance – states, and their interchange through seemingly hysteretic loops (for field along easy axis), with changes for angles close to orthogonality between $\vec{j}$ and $\vec{H}$ were also explained. The coupling field between antiferromagnetic and ferromagnetic layers in the so called "pinned" section was also quantified and verified to be within a range of about 7 Oe, up to a maximum value of 21.54 Oe. This study did not comprise the angles corresponding to $\vec{j} \perp \vec{H}$. A study of sensibility showed the occurence of maximum sensibility for the configuration of current and field antiparalell, and an approximately constant sensibility for all other angles tested.

A multilayer film's magnetoresistance was characterized for variable applied field and orientation within its longitudinal plane. The maximum relative magnetoresistance computed was of about 0.25%, reflecting the importance of this effect in microsensing applications. The saturation resistance was computed, but no $\cos^2 \theta_{\vec{j},\vec{H}}$ dependance could be verified bor angles greater than 90º. The maximum sensibility of the structure was computed for several angles between field and current, and the greatest sensibility occured for 22.5º, suggesting a non-zero angle between the easy axis of the sample and the current. Further studies concerning zero-field resistances with variable angles of rotation of the sample were not conclusive.

Finally, the study of a possible application of these magnetoresistive phenomena was tested – magnetic field sensing. Qualitatively, it was possible to check the reduction of resistance as the test magnets moved away from the sample. However, calibration of the apparatus was not possible, since a calibration curve could not be extracted due to the disappearance of the sample. As a future work, a promising sensing application may be envisaged and planned to the detail.

References

[1] *Protocolos de experiências de Laboratórios de Física II.* pp. 12-14 Department of Physics, Faculty of Sciences of the University of Porto (Feb. 2006).

[2] Ventura J. *Magnetic Nanostructures.* PhD Thesis, Department of Physics, Faculty of Sciences of the University of Porto (Feb. 2006). Accessed via `http://www.fc.up.pt/pessoas/joventur/Tese/MagneticNanostructures.pdf` in 2018/4/25.

[3] Santos J. *Magnetismo e Fenómenos de Transporte com Comportamento Não-Convencional - Filmes Nano-Granulares e Sistemas de Terras Raras com Interacções Competitivas.* PhD Thesis, Department of Physics, Faculty of Sciences of the University of Porto (Jan. 2006), pp.46-50.

[4] Khvalkovsky A. V., Prokhorov A. M. *Гигантское магнитосопротивление: от открытия до Нобелевской премии.* Accessed via `http://www.amtc.ru/publications/articles/2084/?SHOWALL_1=1` in 2018/4/25.

[5] Tian Y., Yan S. *GMR: history, development and beyond.* Science China – Phisics, Mechanics and Astronomy. Vol.56 No.1: 2–14 (Jan. 2013)

[6] Freitas P. P. et al. *Magnetoresistive biochips.* Europhysics News Vol. 34, No. 6 (Nov.-Dec. 2003)

[7] Teixeira J. M. et al. *Versatile, high sensitivity, and automatized angular dependent vectorial Kerr magnetometer for the analysis of nanostructured materials.* Review of Scientiphic Instruments 82, 043902 (2011)